IMPACT DEMAGNETIZATION AT MARS: USING MULTIPLE ALTITUDE MAGNETIC FIELD DATA TO CONSTRAIN PROPERTIES OF CRUSTAL MAGNETIZATION. R. J. Lillis[1], J. S. Halekas[1], K. L. Louzada[2], S. T. Stewart[2] and M. Manga[3]. [1]Space Sciences Laboratory, U. C. Berkeley, Department of Earth and Planetary Sciences, [2]Harvard University, [3]UC Berkeley. Corresponding author's e-mail: rlillis@ssl.berkeley.edu.

Introduction: Mars does not today possess a core dynamo and associated global magnetic field, though strong crustal magnetization implies that one existed in the past [1]. Since the end of the dynamo epoch ~4 Gyr ago [2], large asteroid or comet impacts on Mars in the absence of a magnetizing field have reduced the magnetization of the crust within (and to some extent around) the final impact basins [3].

Within ~0.2-0.8 basin radii, crater excavation removes magnetized material and heating causes thermal demagnetization [4]. Outside this region the shockwave also causes demagnetization; the radius of which is determined by the bulk properties of the crust and mantle, as well as the coercivity of the crustal magnetic minerals [5]. Here we attempt to constrain crustal magnetic properties using simple and models of impact demagnetization of magnetized crust, along with orbital magnetic field data from the Mars Global Surveyor Magnetometer (MAG) at ~400 km, and Electron Reflectometer (ER) at ~185 km.

Observations: the 15 oldest identified Martian impact basins contain substantial magnetization and thus are thought to have formed in the dynamo epoch [2]. On the ~400 km altitude mapping orbit MAG map, only the largest of the younger impact basins Hellas and Argyre show a clearly recognizable demagnetization signature, i.e. low crustal magnetic fields in their centers. This is due to a combination of high altitude and substantial external field contamination (~5-8 nT). The ER map at 185 km is closer to the magnetized crust and much less affected by external fields, yet it contains only ~20 clear impact demagnetization signatures. Why, with ~800 impact basins > 200 km, many if not most of which surely formed after the dynamo ceased, do we not see a stronger correlation between impact basins and magnetic field? Subsequent endogenic processes may have obscured their impact demagnetization patterns, but the answer mostly lies in the non-unique relationship between magnetization and magnetic field, which we model below.

Impact demagnetization modeling. We calculate the magnetic field at the ER and MAG altitudes (185 km and ~400 km) resulting from circular demagnetized (zero magnetization) craters in a 'checker-board' crust. This pattern consists of 3 layers of 15 km-thick square blocks of different uniform lateral extent (to represent average magnetic coherence length). Each block is magnetized with a given magnetization strength (i.e., 5 A/m) directed randomly in one of two opposite directions (consistent with magnetic field polarity reversals).This pattern is shown in the top panel of figure 2 for the Hellas basin. The resulting magnetic field magnitude (|**B**|) at the two desired altitudes are shown in the bottom two panels.

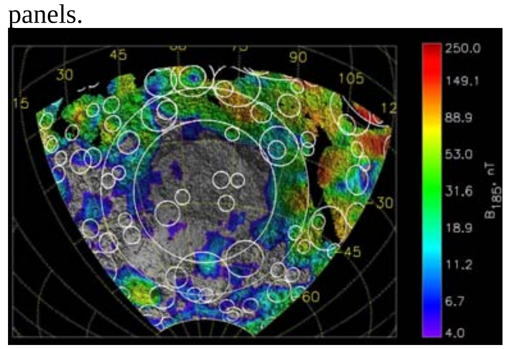

Figure 1: Hellas basin shown on the ER map [6].

Sample case study: Hellas basin. We choose Hellas (2070 km) for a case study because it has a demagnetization signature at both altitudes. The model was run for 5 magnetic inclination angles (0°-90°), 14 lateral coherence scales (25 km-2000 km), 30 magnetization strengths (0.1-100 A/m) and 5 demagnetization diameters (D) of 1800-2800 km. Least-squares fitting was performed jointly on average radial magnetic field profiles at 185 km and 395 km from ER and MAG, in the north half of the basin, ignoring unmagnetized crust to the south.

Results are shown in figure 3. As expected (from the inherent nonuniqueness), these four parameters cannot be separately constrained. The top panel of figure 3 shows how the fit quality varies with magnetization strength and lateral coherence scale. We'll Because we have used 3 layers of (often oppositely) magnetized blocks, even large coherence scales do not result in significant leakage fields into the center of the basin and so are difficult to distinguish from smaller coherence scales. Regardless, the magnetization is constrained in the range ~1.0-10 A/m with the best fit coherence scale being ~400 km. More work is needed with different layering schemes to explore the interplay between vertical and horizontal coherence scales.

The only effect of the magnetic inclination angle in a statistical exercise such as this is to increase slightly the overall magnetic field strength at the inclination angle increases. Since there is a linear relationship between the magnetization strength and the crustal field of altitude, these two parameters are completely non-orthogonal and thus cannot be separated. Therefore this technique can say nothing meaningful about the average magnetic inclination angle, which is not surprising given that we do not use vector information.

Constraints on Hellas' demagnetization diameter. Perhaps the most interesting result from this work is that an effective demagnetization diameter can be found for the Hellas basin. The bottom panel of figure 3 plots the minimum of chi-square across the other three parameters (magnetization strength, lateral coherence scale and magnetic inclination angle) versus the final parameter, the diameter of total demagnetization. There is a very clear minimum around 2440 km; impact demagnetization extends to 1.18 basin radii at Hellas in this model.

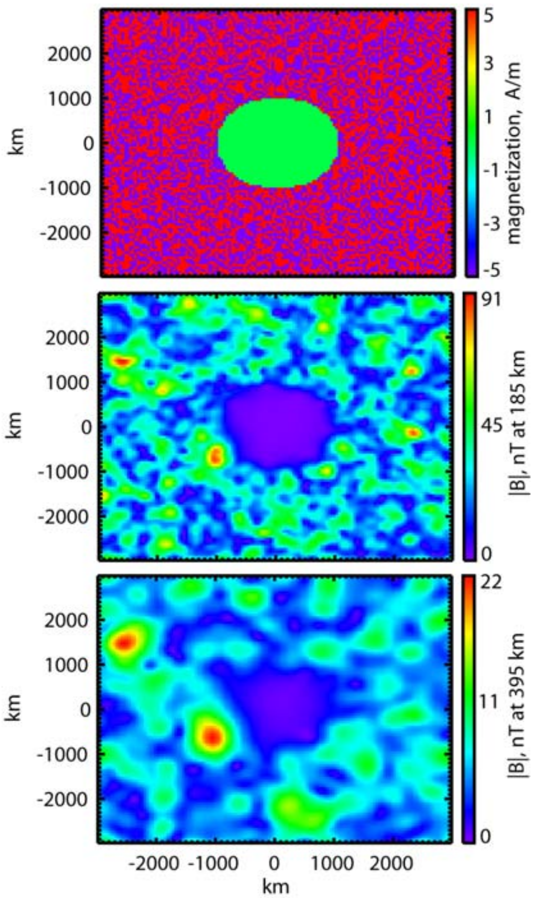

Figure 2: demagnetization model of the Hellas basin (top) and the resulting magnetic field magnitude (|B|) at ER (middle) and MAG (bottom) altitudes.

Future work. We intend to integrate more realistic shock- and thermal-demagnetization curves for various magnetic minerals based on experimental results. We intend to perform three-dimensional numerical simulations of large impacts on Mars using the shock physics code CTH, in order to generate more realistic estimates of the shock temperature and pressure fields in the crust around large craters than have been previously employed [3, 4, 7]. This should allow us to (potentially) place joint constraints on the magnetic carrier and the transient cavity diameter (a poorly understood parameter in basin formation). We also intend to use more realistic crustal magnetization patterns, such as size power law distributions of magnetized blocks.

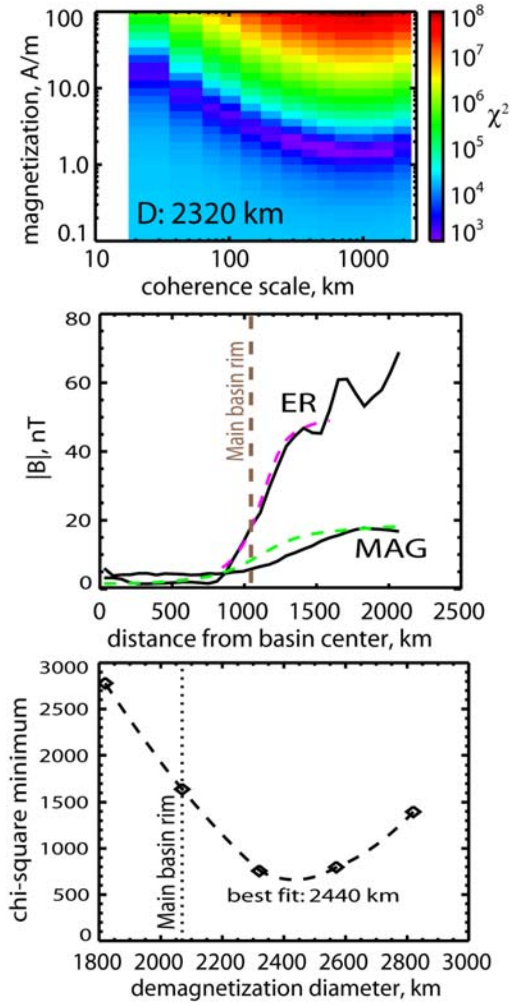

Figure 3: fitting technique applied to Hellas basin. The top panel plots the goodness-of-fit chi-square versus magnetization strength and lateral coherence scale for vertical magnetization and D = 2320 km. Middle panel shows the ER and MAG magnetic field profiles in black with their best fits shown in purple and green respectively. Bottom panel plots goodness-of-fit versus demagnetization diameter.

References: [1] M.H. Acuna et al., *Science* (1999), [2] Lillis et al., GRL (2008) [3] Hood et al., GRL (2003), [4] Mohit and Arkani-Hamed, JGR (2007), [5] Cicowski and Fuller (1978). [6] Lillis at all, Icarus (2008) [7] Kletetschka et al., MAPS (2004)